

Rare-earth triangular lattice spin liquid: a single-crystal study of YbMgGaO_4

Yuesheng Li,¹ Gang Chen,^{2,3,*} Wei Tong,⁴ Li Pi,⁴ Juanjuan Liu,¹
Zhaorong Yang,⁵ Xiaoqun Wang,^{1,6} and Qingming Zhang^{1,6,†}

¹Department of Physics, Renmin University of China, Beijing 100872, P. R. China

²State Key Laboratory of Surface Physics, Center for Field Theory and Particle Physics,
Department of Physics, Fudan University, Shanghai 200433, China

³Collaborative Innovation Center of Advanced Microstructures, Fudan University, Shanghai, 200433, China

⁴High Magnetic Field Laboratory, Hefei Institutes of Physical Science,
Chinese Academy of Sciences, Hefei 230031, P. R. China

⁵Key Laboratory of Materials Physics, Institute of Solid State Physics,
Chinese Academy of Sciences, Hefei 230031, P. R. China

⁶Department of Physics and astronomy, Innovative Center for Advanced Microstructures,
Shanghai Jiao Tong University, Shanghai 200240, P. R. China

(Dated: October 15, 2018)

YbMgGaO_4 , a structurally perfect two-dimensional triangular lattice with odd number of electrons per unit cell and spin-orbit entangled effective spin-1/2 local moments of Yb^{3+} ions, is likely to experimentally realize the quantum spin liquid ground state. We report the first experimental characterization of single crystal YbMgGaO_4 samples. Due to the spin-orbit entanglement, the interaction between the neighboring Yb^{3+} moments depends on the bond orientations and is highly anisotropic in the spin space. We carry out the thermodynamic and the electron spin resonance measurements to confirm the anisotropic nature of the spin interaction as well as to quantitatively determine the couplings. Our result is a first step towards the theoretical understanding of the possible quantum spin liquid ground state in this system and sheds new lights on the search of quantum spin liquids in strong spin-orbit coupled insulators.

PACS numbers: 75.10.Kt, 75.30.Et, 75.30.Gw, 76.30.-v

Introduction.—Recent theoretical advance has extended the Hastings-Oshikawa-Lieb-Schultz-Mattis theorem to the spin-orbit coupled insulators [1–4]. It is shown that as long as the time reversal symmetry is preserved, the ground state of a spin-orbit coupled insulator with odd number of electrons per unit cell must be exotic [1]. This important result indicates that the ground state of strong spin-orbit coupled insulators can be a quantum spin liquid (QSL). QSLs, as we use here, are new phases of matter that are characterized by properties such as quantum number fractionalization, intrinsic topological order, and gapless excitations without symmetry breaking [5, 6]. Among the existing QSL candidate materials [7–33], the majority have a relatively weak spin-orbit coupling (SOC), which only slightly modifies the usual $\text{SU}(2)$ invariant Heisenberg interaction by introducing weak anisotropic spin interactions such as Dzyaloshinskii-Moriya interaction [34–36]. It is likely that the QSL physics in many of these systems mainly originates from the Heisenberg part of the Hamiltonian rather than from the anisotropic interactions due to the weak SOC. The exceptions are the hyperkagome $\text{Na}_4\text{Ir}_3\text{O}_8$ and the pyrochlore quantum spin ice materials where the non-Heisenberg spin interaction due to the strong SOC plays a crucial role in determining the ground state properties [16, 17, 37–48], though both systems contain even number of electrons per unit cell. Therefore, it is desirable to have a QSL candidate system in the spin-orbit coupled insulator that contains odd number electrons per

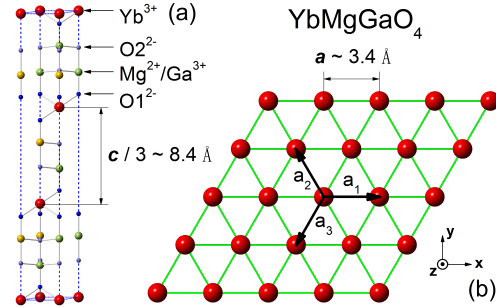


FIG. 1. (Color online.) The YbMgGaO_4 lattice structure (a) and the triangular lattice in the ab plane (b) formed by the Yb^{3+} ions. The inset defines the coordinate system for the spin components.

unit cell, where the strong SOC leads to a non-Heisenberg spin Hamiltonian [37, 38, 40, 48–52].

In this Letter, we propose a possible experimental realization of the QSL with strong SOC and odd number of electrons per unit cell in YbMgGaO_4 , where the Yb^{3+} ions form a perfect triangular lattice (see Fig. 1). It was previously found in a powder sample that the system has a Curie-Weiss temperature $\Theta_{\text{CW}}^{\text{Powder}} \simeq -4\text{K}$ but does not order magnetically down to 60mK [53]. To understand the nature of the obviously disordered ground state observed in YbMgGaO_4 , it is necessary to have a quantitative understanding of the local moments and microscopic

Hamiltonian. We here confirm the effective spin-1/2 nature of the Yb^{3+} local moments at low temperatures from the heat capacity and the magnetic entropy measurements in high-quality single crystal samples. Because the Yb^{3+} ion contains odd number of electrons, the effective spin is described by a Kramers' doublet. Based on this fact, we theoretically derive the symmetry allowed spin Hamiltonian that is non-Heisenberg-like and involves four distinct spin interaction terms because of the strong SOC. Combining the spin susceptibility results along different crystallographic directions and the electron spin resonance (ESR) measurements in single crystal samples, we quantitatively confirm the anisotropic form of the spin interaction. We argue that the QSL physics in YbMgGaO_4 may originate from the anisotropic spin interaction. To our knowledge, YbMgGaO_4 is probably the first strong spin-orbit coupled QSL candidate system that contains odd number of electrons per unit cell with effective spin-1/2 local moments.

Experimental technique.—High-quality single crystals ($\sim 1\text{cm}$) of YbMgGaO_4 , as well as the non-magnetic isostructural material LuMgGaO_4 [54], are synthesized by the floating zone technique. X-ray diffractions (XRD) are performed on the cutting single crystals to confirm the crystallization, the crystallographic orientation and the absence of the impurity phase, and for the single crystal structure refinements [55]. The high quality of the crystallization was confirmed by the narrow XRD rocking curves with $\Delta 2\theta \sim 0.06^\circ$ and 0.04° on ab planes for YbMgGaO_4 and LuMgGaO_4 crystals, respectively. Magnetization ($\sim 60\text{mg}$ of YbMgGaO_4 single crystals) and heat capacity measurements ($10 \sim 20\text{mg}$ of YbMgGaO_4 and LuMgGaO_4 single crystals) were performed using a Quantum design physical property measurement system along and perpendicular to the c axis at $1.8 \sim 400\text{K}$ under $0 \sim 14\text{T}$. The magnetic susceptibilities of single crystals agree with that of powder samples, $\chi_{\parallel}/3 + 2\chi_{\perp}/3 \simeq \chi_{\text{Powder}}$. The ESR measurements ($\sim 60\text{mg}$ of YbMgGaO_4 single crystals) at $1.8 \sim 50\text{K}$ along different crystallographic orientations were performed using a Bruker EMX plus 10/12 CW-spectrometer at X-band frequencies ($f \sim 9.39\text{GHz}$); the spectrometer was equipped with a continuous He gas-flow cryostat.

Kramers' doublet and exchange Hamiltonian.—The Yb^{3+} ion in YbMgGaO_4 has an electron configuration $4f^{13}$, and from the Hund's rules the orbital angular momentum ($L = 3$) and the spin ($s = 1/2$) are entangled, leading to a total angular momentum $J = 7/2$. Under the trigonal crystal electric field, the eight-fold degenerate $J = 7/2$ states are splitted into four Kramers' doublets [38–41, 48]. By fitting the heat capacity results with an activated behavior, we find the local ground state doublet is well separated from the first excited doublet by an energy gap $\Delta \sim 420\text{K}$. This indicates that only the local ground state doublet is active at $T \ll \Delta$. Moreover, the magnetic entropy reaches to a plateau at $\text{Rln}2$

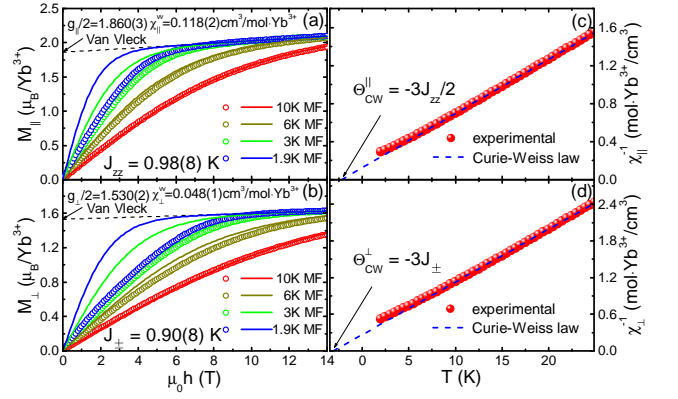


FIG. 2. (Color online.) (a, b) The magnetization of the YbMgGaO_4 single crystals measured at 10, 6, 3 and 1.9K. The dashed lines are linear fits of the experimental results for fields above 12T at 1.9K. The solid curves are the corresponding magnetization calculated by the molecular field approximation. (c, d) The inverse spin susceptibilities (after subtracting the Van Vleck paramagnetism) fitted by the Curie-Weiss law (in dashed lines) for the YbMgGaO_4 single crystals.

per mol Yb^{3+} around 40K, which is consistent with the thermalization of the 2-fold degenerate ground state doublet [53, 54].

As it is analogous to the local moments in the pyrochlore ice systems [27], one can introduce an effective spin-1/2 degree of freedom, \mathbf{S}_i , that acts on the local ground state doublet. The low-temperature magnetic properties are fully captured by these effective spins. Because the $4f$ electron is very localized spatially [28], it is sufficient to keep only the nearest-neighbor interactions in the spin Hamiltonian [56]. Via a standard symmetry analysis, we find the generic spin Hamiltonian that is invariant under the $R\bar{3}m$ space group symmetry of YbMgGaO_4 is given by

$$\mathcal{H} = \sum_{\langle ij \rangle} [J_{zz} S_i^z S_j^z + J_{\pm} (S_i^+ S_j^- + S_i^- S_j^+) + J_{\pm\pm} (\gamma_{ij} S_i^+ S_j^+ + \gamma_{ij}^* S_i^- S_j^-) - \frac{iJ_{z\pm}}{2} (\gamma_{ij}^* S_i^+ S_j^z - \gamma_{ij} S_i^- S_j^z + \langle i \leftrightarrow j \rangle)], \quad (1)$$

where $S_i^{\pm} = S_i^x \pm iS_i^y$, and the phase factor $\gamma_{ij} = 1, e^{i2\pi/3}, e^{-i2\pi/3}$ for the bond ij along the $\mathbf{a}_1, \mathbf{a}_2, \mathbf{a}_3$ direction (see Fig. 1), respectively. This generic Hamiltonian includes all possible microscopic processes that contribute to the nearest-neighbor spin interaction. The highly anisotropic spin interaction in \mathcal{H} is a direct consequence of the spin-orbit entanglement in the local ground state doublet. Moreover, the antisymmetric Dzyaloshinskii-Moriya interaction is prohibited in the Hamiltonian because of the inversion symmetry.

Magnetization and magnetic susceptibility.—In order

to quantitatively determine the exchange couplings, we first perform the magnetization measurements for the YbMgGaO_4 single crystals down to 1.8K under an external magnetic field (from 0T to 14T) parallel and perpendicular to the c axis (see Fig. 1). The Zeeman coupling to the external field is also constrained by the lattice symmetry and is given by [57]

$$\mathcal{H}_Z = -\mu_0\mu_B \sum_i [g_{\perp}(h_x S_i^x + h_y S_i^y) + g_{\parallel}h_{\parallel} S_i^z]. \quad (2)$$

As shown in Fig. 2, the magnetization processes are obtained for both field directions at 1.9K. When the field is above 12T, both magnetizations saturate and become linearly dependent on the field. The slope of the M - H curve is temperature-independent and is understood as the Van Vleck susceptibility ($\chi_{\parallel}^{\text{VV}} = 0.118(2)\text{cm}^3/\text{mol}\cdot\text{Yb}^{3+}$, $\chi_{\perp}^{\text{VV}} = 0.0479(8)\text{cm}^3/\text{mol}\cdot\text{Yb}^{3+}$) that arises from the field-induced electronic transitions [58]. After subtracting the Van Vleck paramagnetic contribution, we obtain the saturated magnetic moments ($g_{\parallel}\mu_B/2$ and $g_{\perp}\mu_B/2$), from which we extract the g factors $g_{\parallel} = 3.721(6)$, $g_{\perp} = 3.060(4)$ [54].

We apply a small external field (0.01T) to measure the spin susceptibilities parallel and perpendicular to the c axis as a function of temperature. At high temperatures ($T \gtrsim 8\text{K}$) both susceptibilities (after the subtraction of Van Vleck paramagnetism) are well fitted by the Curie-Weiss law (see Fig. 2). From the spin Hamiltonian, it is ready to obtain the Curie-Weiss temperatures $\Theta_{\text{CW}}^{\parallel} = -3J_{zz}/2$ ($\Theta_{\text{CW}}^{\perp} = -3J_{\pm}$) for the field parallel (perpendicular) to the c axis. We then use the above relations to find J_{zz} and J_{\pm} . Alternatively, we apply the high-temperature molecular field approximation to fit the field dependence of magnetizations. As shown in Fig. 2, the molecular field result agrees with the experiments very well at 10K. These two approaches together yield $J_{zz} = 0.98(8)\text{K}$ and $J_{\pm} = 0.90(8)\text{K}$.

ESR.—The remaining two coupling constants, $J_{\pm\pm}$ and $J_{z\pm}$, that contribute to the anisotropic spin interaction, completely break the $U(1)$ spin rotation but keep time reversal symmetry intact. They cannot be well resolved by the above thermodynamic measurements. To precisely determine them, we apply the exhaustive ESR measurements and analyze the ESR linewidths. It is well-known that the ESR linewidth is a powerful and direct measure of the anisotropic spin interactions [59–64]. We perform the ESR measurements from 1.8K to 50K along different crystallographic orientations, where the wide ESR signals, as broad as $\mu_0\Delta H(\theta) \sim 0.4\text{T}$, were observed (see Fig. 3, 4 and raw ESR signals [54]).

Here we discuss various sources that broaden the ESR linewidth. The first one is the hyperfine interactions that contribute to the ESR linewidth with $\mu_0\Delta H_h \sim |A_{\parallel}|^2/(g\mu_B|J_0|) \sim 2\text{mT}$ [63], where the hyperfine coupling, $|A_{\parallel}|$, is about 2GHz for Yb^{3+} [65],

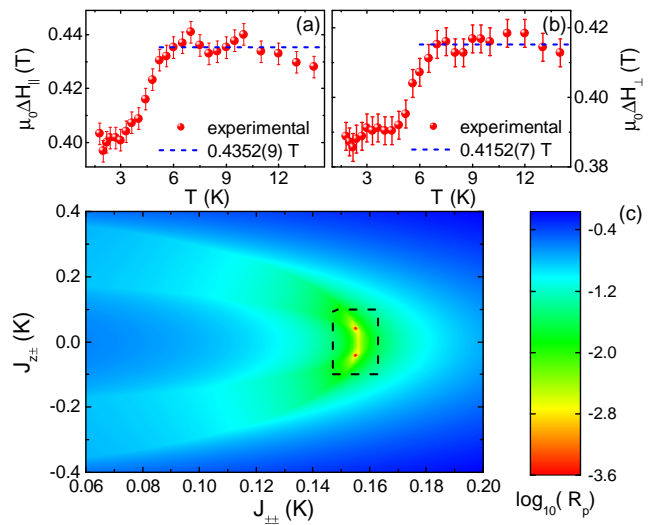


FIG. 3. (Color online.) The temperature dependence of ESR linewidths (a) parallel and (b) perpendicular to the c axis. The dashed lines are the corresponding constant fits to the ESR linewidth data at $T > 6\text{K}$. (c) The deviation, R_p , of the experimental ESR linewidths from the theoretical ones for YbMgGaO_4 . The dashed rectangle gives the optimal parameters $|J_{\pm\pm}| = 0.155(9)\text{K}$ and $|J_{z\pm}| = 0.04(10)\text{K}$.

and J_0 is the isotropic Heisenberg coupling defined as $J_0 \equiv (4J_{\pm} + J_{zz})/3 \sim 1.5(1)\text{K}$ in Eq. (3). The next-nearest-neighbor magnetic dipole-dipole interactions also broaden the ESR signal with $\mu_0\Delta H_d \sim |E_d|^2/(g\mu_B|J_0|) \sim 0.3\text{mT}$ [63]. Here, we have made a maximal estimate of the next-nearest-neighbor dipole-dipole interaction $|E_d|$ as $\mu_0 g^2 \mu_B^2 / [4\pi(\sqrt{3}a)^3]$, where a is the lattice constant. All the Yb^{3+} ions share the same g -tensor, the Zeeman interaction is homogeneous and thus does not contribute to the ESR linewidth [63]. All the above contributions together give an ESR linewidth that is two orders of magnitude smaller than the observed value. To account for such a large ESR linewidth that is $\sim 0.4\text{T}$, the only remaining origin lies in the anisotropy of the nearest-neighbor spin interaction.

We now decompose the spin Hamiltonian in Eq. (1) into the isotropic and the anisotropic parts

$$\mathcal{H} = J_0 \sum_{\langle i,j \rangle} \mathbf{S}_i \cdot \mathbf{S}_j + \mathcal{H}' \quad (3)$$

where J_0 was previously introduced, Γ_{ij} is a traceless coupling matrix, and $\mathcal{H}' = \sum_{\langle i,j \rangle} S_i^{\mu} \Gamma_{ij,\mu\nu} S_j^{\nu}$ is the anisotropic part of the spin interaction. With the Zeeman term in Eq. (2), the ESR linewidth is obtained as

$$\Delta H(\theta) = \frac{(2\pi)^{\frac{1}{2}}}{\mu_B g(\theta)} \left(\frac{M_2^3}{M_4} \right)^{\frac{1}{2}} \quad (4)$$

where θ is the angle between the external field and the c axis, $g(\theta) = (g_{\parallel}^2 \cos^2 \theta + g_{\perp}^2 \sin^2 \theta)^{1/2}$, $M_2 =$

$\langle [\mathcal{H}', M^+][M^-, \mathcal{H}'] \rangle / \langle M^+ M^- \rangle$ is the second moment, and $M_4 = \langle [\mathcal{H}', M^+][\mathcal{H}', M^+] \rangle / \langle M^+ M^- \rangle$ is the fourth moment [62]. Here, $M^\pm \equiv \sum_i S_i^\pm$.

The ESR signal of YbMgGaO₄ single crystal can be well fitted by the first-derivative Lorentzian line shape with a small contribution of dispersion as described by Ref. 64. Both $\mu_0 \Delta H_{\parallel}(T)$ and $\mu_0 \Delta H_{\perp}(T)$ show a gradual broadening [61] with increasing temperature for $k_B T < 5J_0$, and reach almost temperature-independent maxima at $\mu_0 \Delta H_{\parallel} = 0.4352(9)\text{T}$ and $\mu_0 \Delta H_{\perp} = 0.4152(7)\text{T}$ for $k_B T \geq 5J_0$ (see Fig. 3). We fit these high-temperature ESR linewidths according to the theoretical results. In Fig. 3, we plot the deviation of the experimental result from the theoretical one,

$$R_p = \frac{1}{2} \left[\left| \frac{\Delta H_{\parallel} - \Delta H_{\parallel}^{cal}}{\Delta H_{\parallel}} \right| + \left| \frac{\Delta H_{\perp} - \Delta H_{\perp}^{cal}}{\Delta H_{\perp}} \right| \right], \quad (5)$$

as a function of $J_{\pm\pm}$ and $J_{z\pm}$. The optimal fitting is obtained by setting $|J_{\pm\pm}| = 0.155(3)\text{K}$ and $|J_{z\pm}| = 0.04(8)\text{K}$ whose signs cannot be fixed by the fitting.

As an unbiased check of the fitted results, we use the optimal couplings to calculate the angle dependence of the ESR linewidth, $\mu_0 \Delta H^{cal}(\theta)$, where θ is the angle between the external field and the c axis. As shown in Fig. 4, the experimental curve agrees with the theoretical result very well. Moreover, we apply the high-temperature series expansions to compute the spin susceptibilities per Yb³⁺ ion up to $\mathcal{O}(T^{-3})$,

$$\chi_{\parallel} = \frac{\mu_0 g_{\parallel}^2 \mu_B^2}{4k_B T} \left(1 - \frac{3J_{zz}}{2k_B T} - \frac{3J_{\pm\pm}^2 + J_{\pm\pm}^2 + J_{z\pm}^2}{2k_B^2 T^2} + \frac{15J_{zz}^2}{8k_B^2 T^2} \right), \quad (6)$$

$$\chi_{\perp} = \frac{\mu_0 g_{\perp}^2 \mu_B^2}{4k_B T} \left(1 - \frac{3J_{\pm\pm}}{k_B T} + \frac{7J_{\pm\pm}^2}{k_B^2 T^2} - \frac{2J_{\pm\pm}^2}{k_B^2 T^2} - \frac{5J_{z\pm}^2}{16k_B^2 T^2} - \frac{J_{zz}^2}{8k_B^2 T^2} - \frac{J_{\pm} J_{zz}}{4k_B^2 T^2} \right). \quad (7)$$

As we depict in Fig. 4, the high-temperature expansion shows a better fitting with the experimental results at lower temperatures than the simple Curie-Weiss laws.

Discussion.—In the previous powder sample measurements, the magnetic heat capacity of YbMgGaO₄ behaves as $C_v \propto T^\gamma$ ($\gamma \approx 2/3$) from about 1K down to 0.06K [66], suggesting the system is probably in a gapless QSL phase [53]. The residual magnetic entropy of the system at 0.06K is less than 0.6% of the total magnetic entropy [53]. This is a strong indication that we are indeed accessing the ground state property. As far as we are aware of, this is the first clear observation of $C_v \propto T^{2/3}$ in QSL candidate systems. In fact, this behavior is compatible with what one may expect for the U(1) QSL with a spinon Fermi surface in two dimensions [67–69], a state previously proposed for the organic κ -(ET)₂Cu₂(CN)₃ and EtMe₃Sb[Pd(dmit)₂]₂ [67–69]. Although alternative

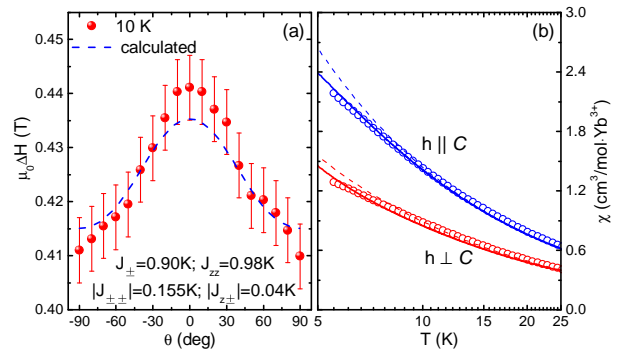


FIG. 4. (Color online.) (a) Angular dependence of ESR linewidth. The dashed curve is the calculated ESR linewidth. (b) The magnetic susceptibilities of YbMgGaO₄ single crystal after subtracting the Van Vleck paramagnetism. The solid curves are the calculated susceptibilities using the high-temperature series expansion. The dashed curves are the Curie-Weiss susceptibilities.

proposals also exist [70], the QSL physics in the organics is believed to originate from the strong charge fluctuation of the weak Mott regime that induces a sizable ring exchange and thus destabilizes the 120° magnetic order for a triangular system [67–69]. In contrast, the physical mechanism to realize possible QSL in YbMgGaO₄ should be rather different. The f electrons of YbMgGaO₄ are very localized and are in the strong Mott regime. The charge fluctuation is very weak and the ring exchange process should be negligible. On the other hand, the anisotropic $J_{\pm\pm}$ and $J_{z\pm}$ spin interaction is a new ingredient brought by the spin-orbit entanglement of the Yb f electrons and is expected to be the physical origin of the QSL physics. This is because in the absence of the anisotropic $J_{\pm\pm}$ and $J_{z\pm}$ spin interaction the antiferromagnetic XXZ model would produce a conventional magnetic order [71]. It is the anisotropic $J_{\pm\pm}$ and $J_{z\pm}$ spin interaction that competes with the XXZ model and may melt the magnetic order in certain parameter regime [72]. Through the current single crystal measurements, we expect YbMgGaO₄ to be a spin-orbit coupled QSL in which the anisotropic spin interaction is the driving force.

To summarize, we have characterized the magnetic properties of large YbMgGaO₄ single crystals that are grown for the first time. The crystal structure and effective spin-1/2 Hamiltonian of YbMgGaO₄ are precisely determined by single crystal X-ray diffractions, thermodynamic measurements and ESR linewidths on the oriented single crystals. We find that the anisotropic spin exchange interaction on the Yb triangular lattice significantly broadens the ESR linewidths. We argue that the anisotropic spin interaction plays an important role to stabilize the possible QSL ground state in YbMgGaO₄. In the future, it will be interesting to numerically study the theoretical model in our work, classify QSLs in strong

spin-orbit coupled insulators, and use inelastic neutron scattering to detect the possible fractionalized spin excitation in the single crystal samples.

Acknowledgement.—We thank Rong Yu for helpful conversation. This work was supported by the NSF of China and the Ministry of Science and Technology of China (973 projects: 2011CBA00112 and 2012CB921701). G.C. was supported by the starting up funds of Fudan University. Q.M.Z. and Y.S.L. was supported by the Fundamental Research Funds for the Central Universities, and the Research Funds of Renmin University of China.

* chggst@gmail.com, former affiliation: Department of Physics, University of Toronto, Ontario, Canada, M5S1A7

† qmzhang@ruc.edu.cn

- [1] H. Watanabe, H. C. Po, A. Vishwanath, and M. P. Zaletel, arXiv:1505.04193.
- [2] M. B. Hastings, Phys. Rev. B **69**, 104431 (2004).
- [3] M. Oshikawa, Phys. Rev. Lett. **84**, 1535 (2000).
- [4] E. H. Lieb, T. Schultz, and D. J. Mattis, Ann. Phys. (N.Y.) **16**, 407 (1961).
- [5] L. Balents, Nature **464**, 199 (2010).
- [6] X.-G. Wen, *Quantum Field Theory of Many-body Systems: From the Origin of Sound to an Origin of Light and Electrons*, reissue ed. (Oxford University Press, New York, USA, 2007).
- [7] Y. Kurosaki, Y. Shimizu, K. Miyagawa, K. Kanoda, and G. Saito, Phys. Rev. Lett. **95**, 177001 (2005).
- [8] T. Itou, A. Oyamada, S. Maegawa, M. Tamura, and R. Kato, Phys. Rev. B **77**, 104413 (2008).
- [9] H. Morita, S. Watanabe, and M. Imada, Journal of the Physical Society of Japan **71**, 2109 (2002).
- [10] Y. Shimizu, K. Miyagawa, K. Kanoda, M. Maesato, and G. Saito, Phys. Rev. Lett. **91**, 107001 (2003).
- [11] S. Yamashita, Y. Nakazawa, M. Oguni, Y. Oshima, H. Nojiri, Y. Shimizu, K. Miyagawa, and K. Kanoda, Nature Physics **4**, 459 (2008).
- [12] T. Itou, A. Oyamada, S. Maegawa, M. Tamura, and R. Kato, Journal of Physics: Condensed Matter **19**, 145247 (2007).
- [13] R. Coldea and *et al*, Phys. Rev. B **68**, 134424 (2003).
- [14] R. Coldea, D. A. Tennant, A. M. Tsvetlik, and Z. Tylczynski, Phys. Rev. Lett. **86**, 1335 (2001).
- [15] S. Nakatsuji and *et al*, Science **309**, 1697 (2005).
- [16] J. S. Gardner, S. R. Dunsiger, B. D. Gaulin, M. J. P. Gingras, J. E. Greedan, R. F. Kiefl, M. D. Lumsden, W. A. MacFarlane, N. P. Raju, J. E. Sonier, I. Swainson, and Z. Tun, Phys. Rev. Lett. **82**, 1012 (1999).
- [17] Y. Okamoto, M. Nohara, H. Aruga-Katori, and H. Takagi, Phys. Rev. Lett. **99**, 137207 (2007).
- [18] Z. Hiroi, M. Hanawa, N. Kobayashi, M. Nohara, H. Takagi, Y. Kato, and M. Takigawa, Journal of the Physical Society of Japan **70**, 3377 (2001).
- [19] M. Yoshida, M. Takigawa, H. Yoshida, Y. Okamoto, and Z. Hiroi, Phys. Rev. Lett. **103**, 077207 (2009).
- [20] Y. Okamoto, H. Yoshida, and Z. Hiroi, J. Phys. Soc. Jpn. **78**, 033701 (2009).
- [21] B. Fåk, E. Kermarrec, L. Messio, B. Bernu, C. Lhuillier, F. Bert, P. Mendels, B. Koteswararao, F. Bouquet, J. Ollivier, A. D. Hillier, A. Amato, R. H. Colman, and A. S. Wills, Phys. Rev. Lett. **109**, 037208 (2012).
- [22] J. S. Helton, K. Matan, M. P. Shores, E. A. Nytko, B. M. Bartlett, Y. Yoshida, Y. Takano, A. Suslov, Y. Qiu, J.-H. Chung, D. G. Nocera, and Y. S. Lee, Phys. Rev. Lett. **98**, 107204 (2007).
- [23] A. Olariu, P. Mendels, F. Bert, F. Duc, J. C. Trombe, M. A. de Vries, and A. Harrison, Phys. Rev. Lett. **100**, 087202 (2008).
- [24] P. Mendels, F. Bert, M. A. de Vries, A. Olariu, A. Harrison, F. Duc, J. C. Trombe, J. S. Lord, A. Amato, and C. Baines, Phys. Rev. Lett. **98**, 077204 (2007).
- [25] J. G. Cheng, G. Li, L. Balicas, J. S. Zhou, J. B. Goodenough, C. Xu, and H. D. Zhou, Phys. Rev. Lett. **107**, 197204 (2011).
- [26] T.-H. Han, J. S. Helton, S. Chu, D. G. Nocera, J. A. Rodriguez-Rivera, C. Broholm, and Y. S. Lee, Nature **492**, 406 (2012).
- [27] H. R. Molavian, M. J. P. Gingras, and B. Canals, Phys. Rev. Lett. **98**, 157204 (2007).
- [28] K. A. Ross, L. Savary, B. D. Gaulin, and L. Balents, Phys. Rev. X **1**, 021002 (2011).
- [29] Y. Li, B. Pan, S. Li, W. Tong, L. Ling, Z. Yang, J. Wang, Z. Chen, Z. Wu, and Q. Zhang, New Journal of Physics **16**, 093011 (2014).
- [30] Y. Li and Q. Zhang, Journal of Physics: Condensed Matter **25**, 026003 (2013).
- [31] Y. Li, J. Fu, Z. Wu, and Q. Zhang, Chemical Physics Letters **570**, 37 (2013).
- [32] S. Bieri, L. Messio, B. Bernu, and C. Lhuillier, Phys. Rev. B **92**, 060407 (2015).
- [33] R. Sibille, E. Lhotel, V. Pomjakushin, C. Baines, T. Fennell, and M. Kenzelmann, Phys. Rev. Lett. **115**, 097202 (2015).
- [34] T. Moriya, Phys. Rev. **120**, 91 (1960).
- [35] T. Moriya, Phys. Rev. Lett. **4**, 228 (1960).
- [36] I. Dzialoshinski, J. Phys. Chem. Solids **4**, 241 (1958).
- [37] G. Chen and L. Balents, Phys. Rev. B **78**, 094403 (2008).
- [38] S. H. Curnoe, Phys. Rev. B **78**, 094418 (2008).
- [39] K. A. Ross, J. P. C. Ruff, C. P. Adams, J. S. Gardner, H. A. Dabkowska, Y. Qiu, J. R. D. Copley, and B. D. Gaulin, Phys. Rev. Lett. **103**, 227202 (2009).
- [40] S. Onoda and Y. Tanaka, Phys. Rev. Lett. **105**, 047201 (2010).
- [41] R. Applegate, N. R. Hayre, R. R. P. Singh, T. Lin, A. G. R. Day, and M. J. P. Gingras, Phys. Rev. Lett. **109**, 097205 (2012).
- [42] A. J. Princep, D. Prabhakaran, A. T. Boothroyd, and D. T. Adroja, Phys. Rev. B **88**, 104421 (2013).
- [43] L.-J. Chang, S. Onoda, Y. Su, Y.-J. Kao, K.-D. Tsuei, Y. Yasui, K. Kakurai, and M. R. Lees, Nature Communications **3**, 992 (2012).
- [44] G. Chen and Y. B. Kim, Phys. Rev. B **87**, 165120 (2013).
- [45] K. Kimura, S. Nakatsuji, J.-J. Wen, C. Broholm, M. B. Stone, E. Nishibori, and H. Sawa, Nature Communications **4**, 1934 (2013).
- [46] J. Reuther, S.-P. Lee, and J. Alicea, Phys. Rev. B **90**, 174417 (2014).
- [47] T. Taniguchi, H. Kadowaki, H. Takatsu, B. Fåk, J. Ollivier, T. Yamazaki, T. J. Sato, H. Yoshizawa, Y. Shimura, T. Sakakibara, T. Hong, K. Goto, L. R. Yaraskavitch, and J. B. Kycia, Phys. Rev. B **87**, 060408

- (2013).
- [48] Y.-P. Huang, G. Chen, and M. Hermele, *Phys. Rev. Lett.* **112**, 167203 (2014).
- [49] W. Witczak-Krempa, G. Chen, Y. B. Kim, and L. Balents, *Annual Review of Condensed Matter Physics* **5**, 57 (2014).
- [50] G. Jackeli and G. Khaliullin, *Phys. Rev. Lett.* **102**, 017205 (2009).
- [51] G. Chen, R. Pereira, and L. Balents, *Phys. Rev. B* **82**, 174440 (2010).
- [52] G. Chen and L. Balents, *Phys. Rev. B* **84**, 094420 (2011).
- [53] Y. Li, H. Liao, Z. Zhang, S. Li, F. Jin, L. Ling, L. Zhang, Y. Zou, L. Pi, Z. Yang, J. Wang, Z. Wu, and Q. Zhang, arXiv:1506.06992.
- [54] See the supplementary material for the detailed information.
- [55] A. Larson and R. Von Dreele, *General Structure Analysis System (GSAS) 2004*, Tech. Rep. (Los Alamos National Laboratory Report LAUR 86-748).
- [56] The further neighbor magnetic dipole interaction is estimated to be much smaller than the nearest neighbor couplings.
- [57] $h_{\perp} \equiv (h_x^2 + h_y^2)^{1/2}$.
- [58] Y. Shirata, H. Tanaka, A. Matsuo, and K. Kindo, *Phys. Rev. Lett.* **108**, 057205 (2012).
- [59] P.-W. Anderson and P. Weiss, *Reviews of Modern Physics* **25**, 269 (1953).
- [60] T. G. Castner and M. S. Seehra, *Phys. Rev. B* **4**, 38 (1971).
- [61] Z. G. Soos, K. T. McGregor, T. T. P. Cheung, and A. J. Silverstein, *Phys. Rev. B* **16**, 3036 (1977).
- [62] A. Zorko, S. Nellutla, J. van Tol, L. C. Brunel, F. Bert, F. Duc, J.-C. Trombe, M. A. de Vries, A. Harrison, and P. Mendels, *Phys. Rev. Lett.* **101**, 026405 (2008).
- [63] B. Pilawa, *Journal of Physics: Condensed Matter* **9**, 3779 (1997).
- [64] H.-A. Krug von Nidda, L. E. Svistov, M. V. Eremin, R. M. Eremina, A. Loidl, V. Kataev, A. Validov, A. Prokofiev, and W. Abmus, *Phys. Rev. B* **65**, 134445 (2002).
- [65] S. K. Misra and S. Isber, *Physica B: Condensed Matter* **253**, 111 (1998).
- [66] We have also measured the heat capacity for the single crystal down to 0.06K, and it does not show any significant difference from the powder sample results.
- [67] O. I. Motrunich, *Phys. Rev. B* **72**, 045105 (2005).
- [68] S.-S. Lee and P. A. Lee, *Phys. Rev. Lett.* **95**, 036403 (2005).
- [69] O. I. Motrunich, *Phys. Rev. B* **73**, 155115 (2006).
- [70] R. V. Mishmash, J. R. Garrison, S. Bieri, and C. Xu, *Phys. Rev. Lett.* **111**, 157203 (2013).
- [71] D. Yamamoto, G. Marmorini, and I. Danshita, *Phys. Rev. Lett.* **112**, 127203 (2014).
- [72] G. Chen and et al, unpublished.